Published in final edited form as:
J Cell Physiol. 2007 March ; 210(3): 807–818. doi:10.1002/jcp.20904.

Thrombospondin-1 Inhibits VEGF Levels in the Ovary Directly by Binding and Internalization Via the Low Density Lipoprotein Receptor-Related Protein-1 (LRP-1)

James Greenaway[1], **Jack Lawler**[2], **Roger Moorehead**[1], **Paul Bornstein**[3], **Jonathan Lamarre**[1], and **Jim Petrik**[1,*]

[1]Department of Biomedical Sciences, University of Guelph, Guelph, Ontario

[2]Beth Israel Deaconess Medical Center and Harvard Medical School, Boston, Massachusetts

[3]Departments of Biochemistry and Medicine, University of Washington, Seattle, Washington

Abstract

VEGF is a potent pro-angiogenic factor whose effects are opposed by a host of anti-angiogenic proteins, including thrombospondin-1 (TSP-1). We have previously shown that VEGF has important extravascular roles in the ovary and that VEGF and TSP-1 are inversely expressed throughout the ovarian cycle. To date, however, a causal interaction between TSP-1 and VEGF has not been identified. Here, we show that TSP-1 has a direct inhibitory effect on VEGF by binding the growth factor and internalizing it via LRP-1. Mice lacking TSP-1 are subfertile and exhibited ovarian hypervascularization and altered ovarian morphology. Treatment of ovarian cells with TSP-1 decreased VEGF levels and rendered the cells more susceptible to TNFα-induced apoptosis. Knockdown of TSP-1, through RNA interference, resulted in overexpression of VEGF and reduced cytokine-induced apoptosis. In conclusion, we demonstrate a direct inhibitory effect of TSP-1 on VEGF in the ovary. TSP-1's regulation of VEGF appears to be an important mediator of ovarian angiogenesis and follicle development.

The growth of normal tissues and pathological structures such as tumors are dependent upon the formation of blood vessels for nutrient delivery and waste removal (Folkman, 1992). Growth of new vasculature is regulated by a balance between pro- and anti-angiogenic factors. A potent pro-angiogenic factor is vascular endothelial growth factor (VEGF), which is a heparin-binding glycoprotein secreted as a homodimer that stimulates endothelial cell proliferation and migration (Bernatchez et al., 2002; Castellon et al., 2002), promotes new vessel formation, increases vascular permeability (Ferrara, 2004), and acts as a survival factor for endothelial cells in vitro and in vivo (Gerber et al., 1998; Jia et al., 2004). In addition to its effects on endothelial cells, we recently reported that VEGF protects ovarian cells from apoptosis by signaling through VEGFR-2 expressed by these cells (Greenaway et al., 2004).

The effects of pro-angiogenic factors are balanced by anti-angiogenic factors such as members of the thrombospondin (TSP) family, which consists of five proteins (TSP-1–5), of which TSP-1 and -2 share structural and functional homology (Bornstein, 1992; Adams and Lawler, 2004). TSP-1 is a secreted glycoprotein located in the extracellular matrix that has been shown to be a potent inhibitor of angiogenesis (Lawler, 2002; Armstrong and Bornstein, 2003;Wang et al., 2003; Cursiefen et al., 2004; Lawler and Detmar, 2004). The

*Correspondence to: Dr. Jim Petrik, University of Guelph, Guelph, Ontario, Canada N1G 2W1. jpetrik@uoguelph.ca.

mechanisms by which the TSPs inhibit angiogenesis are not yet fully understood, although recent work has suggested some possibilities. One mechanism may involve specific interactions with pro-angiogenic factors to inhibit their expression and function. TSP-1 has been shown to maintain an inverse relationship in expression with the potent pro-angiogenic factor, VEGF, in a number of physiological and pathological systems (Detmar, 2000). In addition, a direct interaction of VEGF with TSP-1 and with a TSP-1 type I repeat domain of connective tissue growth factor has been reported (Gupta et al., 1999; Inoki et al., 2002). TSP-1 is also known to bind ligands and interact with the low-density lipoprotein receptor-related protein (LRP-1), resulting in internalization and degradation of the protein (Mikhailenko et al., 1995; Emonard et al., 2004; Wang et al., 2004). LRP-1 is a member of the low-density lipoprotein receptor gene family, which also includes the LDL, VLDL, and apolipoprotein E receptor-2 (Nykjaer and Willnow, 2002; Strickland et al., 2002). These family members are endocytic receptors that regulate the concentration of extracellular ligand by transporting ligand through clathrin-coated pits into intracellular vesicles. LRP-1 is expressed in a host of cell types, including endothelial cells (Yamamoto et al., 1997) and granulosa cells in the ovary (25 Moestrup et al., 1992). Since TSP-1 binds to both LRP-1 and matrix metalloproteinases, it serves to mediate the clearance of MMPs from the extracellular space (Bein and Simons, 2000; Yang et al., 2001). A shared feature of the members of the LDL receptor family is the inhibition of ligand interaction by a 39-kDa receptor-associated protein (RAP). RAP acts as a molecular chaperone and is involved in the folding of lipoprotein receptors, resulting in a conformational change that can prevent ligand binding (Neels et al., 1999; Bu and Marzolo, 2000).

In addition to ligand-binding to pro-angiogenic factors, TSP-1 may also affect vascular formation by inducing endothelial cell apoptosis and inhibiting endothelial cell proliferation in part through its interaction with CD36 (Dawson et al., 1997; Guo et al., 1997; Armstrong and Bornstein, 2003). The signaling pathway that leads to apoptosis includes recruitment of the Src-family tyrosine kinase, $p59^{fyn}$, and the activation of p38 stress kinase and caspases (Jimenez et al., 2000; Yano et al., 2002; Sund et al., 2005). While stimulating endothelial cell apoptosis, TSP-1 simultaneously inhibits proliferative and migratory influences of other molecules such as estrogen (Sengupta et al., 2004).

The ovary provides a unique opportunity to study angiogenic processes, as it is one of the few tissues in the adult that undergoes repetitive blood vessel formation, maturation, and regression (Tsafriri, 1995). We have shown previously that TSP-1 and VEGF are inversely expressed, with VEGF expression levels increasing throughout ovarian follicle development, and TSP-1 levels decreasing as follicle progression occurs (Petrik et al., 2002; Greenaway et al., 2004). This inverse relationship has been seen in other normal systems and also in pathological conditions, such as in tumor formation, where VEGF levels are elevated and TSP-1 expression is reduced (Doll et al., 2001; Kwak et al., 2002). In experimental tumors in which TSP-1 expression is reduced, VEGF increases to a level where it can override the inhibitory effect of TSP-1 on angiogenesis (Gonzalez et al., 2004; Fontana et al., 2005). TSP-1 has also been implicated as a functional mediator of the anti-angiogenic effect of chronic low-dose metronomic chemotherapeutic approaches (Bocci et al., 2003; Kerbel and Kamen, 2004). Although an inverse relationship has been observed in a number of physiological systems, a characterization of the interaction between TSP-1 and VEGF has not been performed.

The generation of TSP-1-null mice has further illuminated the importance of this protein in inhibiting angiogenesis. TSP-1-null mice demonstrate significantly increased retinal vascularization (Wang et al., 2003) and display two to threefold increase in tumor growth rates (Lawler et al., 2001; Sund et al., 2005). Interestingly, these mice also have reduced litter size, suggesting reproductive dysfunction (Lawler et al., 1998).

This study characterizes the ovarian morphology of TSP-1 null mice and identifies mechanisms by which TSP-1 might directly influence VEGF levels in the ovary.

EXPERIMENTAL PROCEDURES

Cell lines and tissue collection

Spontaneously immortalized rat granulosa cells (SIGC) were a generous gift from Dr. Robert Burghardt (Texas A&M University, College Station, TX). $LRP1^+$ and $LRP1^-$ Chinese hamster ovary (CHO) cells were kindly donated by Dr. David Fitzgerald (NCI, Bethesda MD). SIGC were cultured in DMEM/F12 supplemented with 10% FBS and 2% penicillin/streptomycin (Life Technologies, Grand Island, NY) and treated as described below. CHO cells were maintained in DMEM supplemented with 10% FBS and 2% penicillin/streptomycin (Life Technologies) and treated as described below. Murine microvascular endothelial cells (ATCC Number CRL-2586) were purchased from the American Type Culture Collection (ATCC, Manassus, VA) and maintained in DMEM supplemented with 10% FBS and 2% penicillin/streptomycin (Life Technologies).

TSP-1-null mice were generated as described previously and backcrossed eight times to the C57Bl-6 background (Lawler et al., 1998). Ovaries were removed via laparotomy, with one ovary being immersed immediately in liquid nitrogen and stored at −80°C for protein isolation, and the other ovary fixed overnight in 10% (vol/vol) neutral-buffered formalin at 4°C for immunohistochemistry/immunofluorescence experiments.

Small interfering RNA and transfection reagents

Stealth™ siRNA targeting TSP-1 (BLOCK-IT™ RNAi Express; 1299003) and negative control siRNAs were purchased from Invitrogen. Negative controls included in this study were vehicle control and Stealth™ RNAi Negative Control with medium GC content (Invitrogen). Cells were transfected with siRNAs using lipofectamine 2000 (Invitrogen) in Opti-MEM.

Transfection of small interfering RNAs

SIGC were plated in DMEM-F12 at a density of 2×10^5 cells/5 ml in 60-mm dishes or 1×10^5 cells/2 ml DMEM-F12 on glass coverslips in six-well plates. At approximately 50% confluence, cells were transfected with 200 nmol/L siRNA in lipofectamine 2000 reagent according to the manufacturer's instructions. Briefly, 20 μl lipofectamine 2000 was diluted in 500 μl Opti-MEM and incubated for 5 min at room temperature. In a separate tube, 10 μl of 50 μmol/L siRNA was diluted in 450 μl of Opti-MEM. Diluted oligofectamine (250 μl) was added to the diluted siRNA and the complex was incubated for 20 min at room temperature. Cells were washed in Opti-MEM and 1.5 ml Opti-MEM was added to each 60-mm dish and 500 μl Opti-MEM was added to each well of the 6-well plates. siRNA + Opti-MEM complexes (500 μl) were added to each dish/well. The final concentration of the siRNA was 200 nmol/L. After 6 h, 2 ml of DMEM-F12 with 10% FBS was added without removing the transfection media. Transfections were allowed to continue for 48 h. Transfection controls included medium controls (cells in Opti-MEM), vehicle controls (20 μl lipofectamine 2000 in 500 μl Opti-MEM) and transfection with negative control siRNA (Stealth™ RNAi Negative Control scrambled sequence with medium GC content) as described.

Immunohistochemistry/immunofluorescence

Five micrometer-thick paraffin embedded ovarian tissue sections from TSP-1-null and wild-type (C57BL-6) mice were incubated for 24 h at 4°C in a humidified chamber with mouse anti-CD31 (1:500 dilution; Pharmingen, Mississauga, ON), rabbit polyclonal anti-VEGF

(1:600 dilution; Santa Cruz Biotechnology, CA), or rabbit polyclonal anti-VEGFR-2 (1:500 dilution, Sigma, Oakville, ON). Antisera were diluted in 0.01 PBS (pH 7.5) containing 2% (wt/vol) BSA and 0.01% (wt/vol) sodium azide (100 μl/slide). All subsequent incubations were at room temperature. Biotinylated anti-mouse or anti-rabbit IgGs (both 1:100 dilution; Vector Laboratories, Burlingame, CA) were diluted in the same buffer and applied for 2 h. The slides were then washed in PBS and incubated with avidin and biotinylated horseradish peroxidase (1:30 dilution) (Extravidin, Sigma). Peptide immunoreactivity was localized by incubation in fresh diaminobenzidine tetrahydrochloride (DAB tablets, 10 mg, Sigma) with 0.03% (vol/vol) hydrogen peroxide for 2 min. Tissue sections were counterstained with Carazzi's Hematoxylin for 1 min. The percentage of immunopositive versus immunonegative follicular cells was calculated with integrated morphometry software (Metamorph, Universal Imaging Inc., California).

For immunofluorescence experiments, SIGC were cultured to approximately 80% confluence on glass coverslips housed in 6-well dishes. SIGC were serum-starved and treated with 50 ng/ml VEGF, or 100 ng/ml TSP-1, or a combination of VEGF and TSP-1, overnight. After treatment, cells were fixed in 10% neutral buffered formalin and permeabilized in 0.1% Triton X-100 (Sigma) for 15 min at room temperature. Cells were blocked in PBS containing 5% (wt/vol) bovine serum albumin (BSA) and 0.01% (wt/vol) sodium azide and then primary antibodies (VEGF, 1:600 dilution, Santa Cruz; VEGFR2, 1:500 dilution, Santa Cruz; proliferating cell nuclear antigen (PCNA), 1:600 dilution, Sigma; Bcl-2, 1:500 dilution, Santa Cruz; Fas, 1:600 dilution, Pharmingen) were added to slides overnight at 4°C. Secondary antibodies, conjugated to Alexa Fluor 488 or Alexa Fluor 594 dyes (Molecular Probes, Invitrogen, Burlington, ON), were added for 2 h at room temperature, followed with application of antifade (ProLong Gold, Molecular Probes). Cells were imaged with an inverted Olympus microscope using phase contrast to demonstrate cell morphology. Fluorescence staining was captured, and overlay of immunofluorescence and phase contrast images was performed using integrated morphometry software (Metamorph).

To establish specificity of staining in histology and fluorescence experiments, the primary antiserum was substituted with non-immune serum and secondary antibody was omitted. In each case, staining was abolished.

Detection of apoptosis

To determine the effect of TSP-1 on granulosa cell apoptosis, SIGC were cultured to 90% confluence on coverslips, serum starved overnight and then cultured in the presence or absence of 100 ng/ml TNFα (which we have previously shown to be an effective inducer of apoptosis in these cells (7)), 50 ng/ml VEGF and increasing concentrations of purified TSP-1 (10, 50, 100, 1,000 ng/ml) for 6 h. After treatment, cells were washed and fixed in 10% (vol/vol) neutral buffered formalin. To evaluate the effect of TSP-1 knockdown on SIGC apoptosis, TSP-1 RNAi experiments were conducted as described above. Cells either remained untreated in serum-free DMEM-F12, or were subjected to cytokine challenge (100 ng/ml TNFα) in the presence or absence of 50 ng/ml VEGF for 6 h. After treatment, cells were fixed in 10% (vol/vol) neutral buffered formalin overnight at 4°C. Detection of immunofluorescence in apoptotic cells was performed using a TUNEL assay according to manufacturer's instructions (Roche Applied Science, Laval, Quebec). Briefly, after fixation cells were permeabilized in 0.1% (vol/vol) Triton X-100 (Sigma), washed in PBS and incubated with the FITC-conjugated TUNEL enzyme for 60 min to detect DNA fragmentation. Nuclei were counterstained with DAPI and imaged with an Olympus BX-61 microscope and integrated morphometry software (Metamorph). For analysis, 10 fields of view at magnification 250× were quantified in each experiment (n = 3). Apoptosis was quantified as the percentage of TUNEL-positive cells.

Western blotting

Twenty microgram of total protein extracted from TSP-1-null and wild-type ovarian lysates and from cells subjected to TSP-1 RNAi was run on an 8% SDS–PAGE separating gel. Commercially available VEGF protein standard (Santa Cruz Biotechnology) was used as positive control for blots probing for VEGF. The separated proteins were electro-transferred to PVDF membrane (Millipore, Billerica, MA). Membranes were blocked overnight with 5% (wt/vol) skim milk at 4°C and then were incubated for 2 h at room temperature with rabbit polyclonal anti-VEGF (1:600 dilution, Santa Cruz) or mouse monoclonal anti-TSP-1 (1:500 dilution, Abcam, Cambridge, MA) on a rocking platform. After washing with TTBS (TBS, 1% (vol/vol) Tween 20) and re-blocking, blots were incubated with peroxidase-conjugated anti-rabbit secondary antibody (1:1,000 dilution; Vector Laboratories) or anti-mouse IgG (1:1,000 dilution, Vector Laboratories) for 1 h at room temperature on a rocking platform. Reactive protein was detected with ECL chemiluminescence (Boehringer Manheim, MD) and Konica medical X-ray film (Wayne, NJ). After ECL detection, membranes were probed with α-tubulin antibody (1:1,000 dilution, Santa Cruz) and finally stained with Coomassie Blue to ensure equal protein load.

Cell binding and internalization assays

Purified human VEGF (R&D Systems, MN) and human TSP-1 (Sigma) were fluorescently-labeled with Alexa Fluor 488 Protein Labeling Kit (Molecular Probes) according to the manufacturer's instructions. After conjugation of the proteins, SIGC (approximately 90% confluent) were cultured in the presence of labeled VEGF (50 ng/ml) or TSP-1 (100 ng/ml) overnight in serum-free DMEM/F12. For labeled VEGF, unlabeled purified TSP-1 (100 ng/ml) was also added to media, and for labeled TSP-1, unlabeled VEGF (50 ng/ml) was added. Following treatment, SIGC were fixed with 10% (vol/vol) neutral buffered formalin at room temperature for 1 h, followed by PBS washes. Immunofluorescence experiments were performed as described above with VEGF-treated SIGC incubated overnight with a goat polyclonal anti-TSP-1 antibody (1:500 dilution; Santa Cruz) and TSP-1-treated SIGC incubated with a rabbit polyclonal anti-VEGF antibody (1:600 dilution, Santa Cruz). Protein and antibody localization and co-localization was determined with laser scanning confocal microscopy (Olympus Fluoview 500 scanning confocal microscope) and integrated morphometric analysis (Image Pro Plus, MediaCybernetics, SanDiego, CA).

To determine whether TSP-1-mediated internalization of VEGF occurred through the LRP-1, initial experiments were performed on LRP-1-positive and LRP-1-negative CHO cells. To evaluate the role of LRP-1 in TSP-1-mediated VEGF internalization in granulosa cells, the above protein labeling and internalization experiment was repeated on SIGC and murine microvascular endothelial cells (mEC) that either remained unconditioned or were pre-treated with 500 nM RAP. RAP is a known antagonist of LRP-1 and prevents ligand binding to the receptor (Bu and Marzolo, 2000; Lazic et al., 2003). Human RAP was expressed in bacteria as a fusion protein with glutathione S-transferase. The RAP-GST fusion protein was prepared and purified as described previously (Laithwaite et al., 2001).

SIGC, mEC, and LRP-positive and -negative CHO cells were seeded into 12-well dishes (Corning, NY) at 1×10^5 cells/well 24 h prior to the assay in DMEM/F12 at 37°C, and 5% CO_2 in air. After incubation, cells were cultured with 1 nM ^{125}I VEGF (Amersham Life Sciences, Oakville, ON) for the times indicated (15, 30, 60, 90, 120, 150, 300 min) in the absence or presence of 500 nM RAP. After incubation, cells were washed in PBS and released with trypsin (50 μg/ml) and proteinase K (50 μg/ml) in buffer (containing 5 mM EDTA). Internalized isotope was measured with a gamma counter and corrected by subtracting the amount of degradation products present in the absence of cells.

Statistical analysis

Results are reported as mean ± standard error of the mean (SEM). For densitometric analysis of immunoblots, statistical differences between groups were measured with 2-way analysis of variance (ANOVA), followed by Tukey's post-hoc tests for individual differences when indicated by ANOVA ($\alpha = 0.05$). For in vitro experiments, data were collected from three independent cultures for each treatment group, each in triplicate. For morphometric analysis of histologic images, six separate follicles from TSP-1-null and wild-type mice were used and the entire follicle was included in the analysis. One-way ANOVA, followed by Bonferroni's test for differences between means was used to assess statistical differences between the percentage of immunopositive follicular and cultured cells. Data were analyzed using SAS statistical analysis software (SAS Institute, Cary, NC). The level of significance was set at $P < 0.05$.

RESULTS

Follicle and vascular morphology is altered in TSP-1-null mice

Using integrated morphometric image analysis software (MetaMorph), ovarian follicle number and size were quantified from paraffin-embedded ovaries from wild-type and TSP-1-null mice. TSP-1-null mice exhibited a significant ($P < 0.05$) increase in the number of both pre-antral and antral follicles (Table 1). Along with the increase in follicle number, the mean antral follicle size was reduced in TSP-1 null mice (36 ± 4 μm) compared to wild-type controls (44 ± 6 μm) (Table 1). To determine changes in ovarian vasculature, ovaries from wild-type and TSP-1-null mice were immunostained with an anti-mouse CD31 antibody, which specifically stains endothelial cells (Fig. 1A). Ovarian vessel density was calculated as the area of CD31-positive blood vessels divided by the total tissue area. TSP-1-null mice demonstrated a threefold ($P < 0.05$) increase in ovarian blood vessel density, compared to controls (Fig. 1C). In addition to increased vessel density, there was a significant increase in CD31 protein in whole ovary homogenates in TSP-1-null mice, compared to controls (Fig. 1B).

Ovaries of TSP-1-null mice express elevated levels of VEGF

Ovaries were collected from TSP-1 null and wild-type mice and subjected to immunohistochemistry and Western blot analysis. TSP-1 null ovaries exhibited an increase in VEGF staining, which was primarily localized to endothelial, granulosa, and theca cells (Fig. 2A). Western blot analysis demonstrated a significant ($P < 0.05$) increase in VEGF protein in ovaries from TSP-1 null mice compared to wild-type controls (Fig. 2B).

TSP-1 reduces VEGF levels in granulosa cells and induces apoptosis

To evaluate whether TSP-1 has a direct inhibitory effect on VEGF levels, SIGC were cultured in the absence or presence of purified TSP-1 at varying concentrations (10, 50, 100, 1,000 ng/ml). Treatment at 50 and 100 ng/ml significantly ($P < 0.05$) reduced VEGF protein levels, compared to untreated cells (Fig. 3A). As our previous studies show that VEGF is a potent cytoprotective factor for granulosa cells (Greenaway et al., 2004), we wanted to evaluate whether the TSP-1-induced reduction in VEGF levels would make the SIGC more vulnerable to TNFα challenge. Serum-starved, VEGF-treated SIGC were more vulnerable ($P < 0.05$) to 100 ng/ml TNFα in the presence of 100 or 1,000 ng/ml TSP-1 (Fig. 3B).

TSP-1 alters the expression of proliferative and apoptotic proteins in vitro

Immunofluorescence (Fig. 4A,B) and immunoblot (Fig. 4C) experiments were performed on untreated SIGC, and those treated either with 100 ng/ml TSP-1 alone or with 100 ng/ml TSP-1 and 50 ng/ml VEGF. TSP-1 100 ng/ml significantly reduced the levels of VEGF and

its main signaling receptor, VEGFR2 (Fig. 4). Concomitant treatment of 100 ng/ml TSP-1 and 50 ng/ml VEGF resulted in levels of VEGF and VEGF R2 similar to that of controls. The rate of granulosa cell proliferation, as determined by PCNA expression, was unchanged by TSP-1 or combination treatment (Fig. 4). Expression of cytoprotective proto-oncogene bcl-2 was reduced after treatment with TSP-1, while concurrent treatment with both TSP-1 and VEGF resulted in bcl-2 levels similar to controls (Fig. 4). Conversely, exposing SIGC to 100 ng/ml TSP-1 significantly ($P < 0.05$) increased expression of pro-apoptotic Fas (Fig. 4), and this increase was reversed when cells were cultured in the presence of both TSP-1 and VEGF.

TSP-1 binds VEGF resulting in internalization by LRP-1

The above experiments demonstrate that TSP-1 has an inhibitory influence on VEGF levels in SIGC. TSP-1 has been shown to bind VEGF (Gupta et al., 1999) and we wanted to determine whether a mechanism by which TSP-1 inhibited VEGF levels was through binding and internalization via LRP-1. To evaluate whether TSP-1 acted as a molecular linker that formed a complex with VEGF, which was in turn internalized by LRP-1, we performed reciprocal fluorochrome labeling of TSP-1 and VEGF. Internalization was followed in the presence or absence of the LRP-1 antagonist, RAP, and in CHO cells known to possess or be deficient in LRP-1. In LRP-1-positive CHO cells, TSP-1 and VEGF co-localized intracellularly following co-incubation, whereas internalization did not occur in LRP-negative CHO cells (data not shown). In SIGC, labeled TSP-1 co-localized intracellularly with VEGF (Fig. 5A). Reciprocal experiments showed that labeled VEGF co-localized with TSP-1 in cultured granulosa cells (Fig. 5A). This internalization was abolished in the presence of 500 nM RAP (Fig. 5A). In another labeling experiment, labeled TSP-1 co-localized with VEGF in LRP-1-positive CHO cells, whereas no internalization was visible in LRP-deficient CHO cells (data not shown). Using ^{125}I labeled VEGF, SIGC, mEC and LRP-1+ CHO cells accumulated maximal isotope by approximately 90 min in culture, at which time radioactivity began to diminish (Fig. 5B). In LRP-1-deficient CHO cells or in the presence of 500 nM RAP, however, ^{125}I VEGF was not internalized throughout the culture period (Fig. 5B). RNA interference of TSP-1 also inhibited 125I-VEGF internalization (Fig. 5B), as described in more detail below.

TSP-1 knockdown increases VEGF levels and inhibits VEGF internalization

SIGC were transfected with siRNA directed against TSP-1 to specifically address whether TSP-1 directly affected VEGF levels in granulosa cells and to evaluate the role of TSP-1 in VEGF internalization. Figure 6A and B show immunofluorescence and Western blot analyses of SIGC after 48 h transfection with vehicle control, RNAi control, and TSP-1 RNAi constructs. TSP-1 RNA interference resulted in approximately an 80% reduction in protein expression by SIGC, as determined by immunofluorescence staining and integrated morphometry analysis (data not shown). TSP-1 protein levels in cells transfected with vehicle or RNAi control were similar to TSP-1 expression in non-transfected cells. In cells transfected with TSP-1 siRNA, there was a significant increase in VEGF, as identified by immunofluorescence (Fig. 6A) and by Western blot analysis (Fig. 6B). TSP-1 knockdown resulted in a significant increase in VEGF expression. As we know that VEGF is cytoprotective for granulosa cells, we wanted to determine the effect of TSP-1 inhibition on SIGC's response to cytokine-induced apoptosis. Serum starvation resulted in a basal apoptotic rate of approximately 16 ± 5% (Fig. 6C). Exposure to 100 ng/ml TNFα caused a significant ($P < 0.05$) increase in apoptosis, with 62 ± 14% of the cells dying. When VEGF (50 ng/ml) was added, together with vehicle, and in RNAi control transfections, the incidence of apoptosis decreased to 15 ± 7% and 14 ± 5%, respectively. There was a further significant ($P < 0.05$) reduction in apoptosis (5 ± 3%) in SIGC transfected with TSP-1 siRNA (Fig. 6C). We have shown that TSP-1 binds and internalizes VEGF (Fig. 5), possibly

contributing to the reduced VEGF expression that occurs following exposure to TSP-1 (Fig. 3). We performed labeling and internalization experiments on SIGC that had TSP-1 knocked down through RNA interference to determine whether VEGF internalization occurred through TSP-1 specifically. In SIGC subjected to TSP-1 RNAi, there was a reduction in VEGF internalization of approximately 80%, compared to untreated SIGC (Fig. 5B), which corresponded to the approximate 80% reduction in TSP-1 expression due to RNAi.

DISCUSSION

Regulation of angiogenesis requires a complex interaction between pro- and anti-angiogenic factors. Disruption of this balance can result in vascular disorders that contribute to pathologies such as tumor formation (Scharovsky et al., 2004; Nyberg et al., 2005). In the ovary, follicular development and function are inherently dependent upon vascularization, which occurs in a tightly regulated fashion. Avascular primordial follicles rely on nutrient delivery from the stroma (Fraser and Wulff, 2001). After recruitment and initial development of a primary follicle, a distinct thecal cell layer is formed and endothelial cells are recruited from neighboring blood vessels in the stroma (Barboni et al., 2000). As the follicle progresses to the antral phase, blood vessel formation continues in the thecal layer and angiogenic growth into the avascular granulosa cell layer is prevented by its basement membrane. As the follicle continues to grow, approximately 25%–30% of proliferating cells are endothelial cells that are extending the vascular network within the thecal layer (Fraser and Wulff, 2001). It is thought that the level of vascularization may be a decisive factor in selection of the dominant follicle by increasing the supply of nutrients, growth factors, and hormones, and therefore supporting the growth of the dominant follicle (Berisha et al., 2000; Zimmermann et al., 2001). After ovulation occurs, the follicle wall collapses, the granulosa cell layer involutes, and there is a disintegration of the basement membrane (Tsukada et al., 1996). These early luteal events are accompanied by differentiation of the thecal and granulosa cells into steroidogenically active luteal cells and an invasion of new blood vessels that develop from pre-existing vasculature. This explosive increase in angiogenesis continues so that by the midluteal phase, virtually every differentiated luteal cell is in contact with the endothelium. As a result, the mature corpus luteum is reported to have the highest blood flow of any tissue in the body (Wiltbank et al., 1988).

In addition to the known angiogenic effects of VEGF in the ovary, we have previously demonstrated that ovarian granulosa cells express the VEGF kinase receptor VEGFR-2 (Flk-1) (Greenaway et al., 2004). Results from the current study show that the loss of the inhibitory effect of TSP-1 in TSP-1-null mice results in increased levels of follicular VEGF. VEGF exerts a cytoprotective effect on granulosa cells during growth and development of the follicle and the elevated VEGF present may elicit a stronger cytoprotective effect on the granulosa cells, inhibiting granulosa cell apoptosis which is a necessary component of follicle atresia (Wulff et al., 2002; Manabe et al., 2004; Valdez et al., 2005). Reduced follicle atresia may contribute to the increase in follicle number seen in the TSP-1 null mice in the present study. In the polycystic ovarian syndrome (PCOS) there are elevated ovarian and serum VEGF levels, and this overexpression is associated with an increase in the number of ovarian follicles and reduced follicle atresia (Jonard et al., 2005). The expression levels of TSP-1 in PCOS and the potential role of VEGF as a cytoprotective agent in this disease have not yet been determined.

TSP-1 is a scavenger for fibroblast growth factor (FGF)-2 (Margosio et al., 2003) and is known to bind VEGF (Gupta et al., 1999). Our study demonstrates that TSP-1 is internalized via LRP. These results agree with others that have shown that TSP-1 is not degraded in cells deficient in LRP (Godyna et al., 1995; Mikhailenko et al., 1997) and that catabolism of TSP-1 is inhibited by RAP (Margosio et al., 2003). We determined in this study that TSP-1

bound VEGF and internalized it via LRP in our granulosa and endothelial cells, demonstrating that LRP is an essential mediator of the catabolism of the complex. These results suggest that in the ovary, TSP-1 may have a bimodal effect. TSP-1 may exert a classical anti-angiogenic effect by binding and internalizing VEGF in endothelial cells, but may have an important extravascular role as well. As VEGF is a potent mitogen (Li et al., 2005) and survival factor (Pauli et al., 2005) for endothelial cells, the reduced bioavailability of the factor would significantly reduce the pro-angiogenic stimulus. As we have shown previously (Greenaway et al., 2004, 2005), VEGF has a very important extravascular cytoprotective role in granulosa cells. The anti-VEGF effect of TSP-1 in ovarian cells may have a significant influence on ovarian morphometry and function. Our TSP-1 null mice demonstrate elevated ovarian VEGF levels, likely due to loss of inhibitory influence of TSP-1. Concurrent with the overexpression of VEGF, the ovaries of TSP-1 null mice had an increase in follicle number, which is consistent with our previous findings that VEGF inhibits granulosa cell death and follicle atresia (Greenaway et al., 2004, 2005). Reduced atresia would be an important factor contributing to the development of a greater than normal number of antral follicles, as is seen in PCOS. Along with its inhibitory influence on VEGF, TSP-1 also inhibited expression of VEGFR-2 in cultured granulosa cells. Although the mechanism for this inhibition is not yet known, the reduced VEGFR-2 expression may be secondary to the lower levels of VEGF, as VEGF is known to regulate the expression of VEGFR-2 in an autocrine and paracrine fashion (Vacca et al., 2003).

Knockdown of TSP-1 in vitro and in vivo resulted in an increase in VEGF levels in the current study. The increased VEGF in the ovaries of TSP-1 null mice may be responsible for the dramatic ovarian hypervascularization, which is similar to that seen in different tumors associated with elevated VEGF expression. This increased blood vessel density mirrors the hypervascularization seen in ovarian tumors that are associated with poor clinical outcome and disease progression (Shen et al., 2000; Amis et al., 2005).

In conclusion, the present study demonstrates a significant increase in ovarian VEGF levels, hypervascularization, and altered ovarian morphology in mice lacking the TSP-1 gene. TSP-1 directly inhibits VEGF expression at least partly through binding to the growth factor and cellular internalization through the LRP receptor. Other potential inhibitory mechanisms remain to be investigated. The results from this study provide insight into regulatory mechanisms that may be important in mediating ovarian vasculature and ovarian cell survival.

Acknowledgments

We thank Michelle Ross and Katrina Watson for excellent technical assistance.

Contract grant sponsor: Natural Sciences and Engineering Research Council of Canada; Contract grant sponsor: Ontario Cancer Research Network; Contract grant number: 047142; Contract grant sponsor: NIH; Contract grant number: HL68003.

LITERATURE CITED

Adams JC, Lawler J. The thrombospondins. Int J Biochem Cell Biol. 2004; 36:961–968. [PubMed: 15094109]

Amis SJ, Coulter-Smith SD, Crow JC, Maclean AB, Perrett CW. Micro-vessel quantification in benign and malignant ovarian tumors. Int J Gynecol Cancer. 2005; 15:58–65. [PubMed: 15670298]

Armstrong LC, Bornstein P. Thrombospondins 1 and 2 function as inhibitors of angiogenesis. Matrix Biol. 2003; 22:63–71. [PubMed: 12714043]

Barboni B, Turriani M, Galeati G, Spinaci M, Bacci ML, Forni M, Mattioli M. Vascular endothelial growth factor production in growing pig antral follicles. Biol Reprod. 2000; 63:858–864. [PubMed: 10952932]

Bein K, Simons M. Thrombospondin type 1 repeats interact with matrix metalloproteinase 2. Regulation of metalloproteinase activity. J Biol Chem. 2000; 275:32164–32173.

Berisha B, Schams D, Kosmann M, Amselgruber W, Einspanier R. Expression and localisation of vascular endothelial growth factor and basic fibroblast growth factor during the final growth of bovine ovarian follicles. J Endocrinol. 2000; 167:371–382. [PubMed: 11115764]

Bernatchez PN, Rollin S, Soker S, Sirois MG. Relative effects of VEGF-A and VEGF-C on endothelial cell proliferation, migration and PAF synthesis: Role of neuropilin-1. J Cell Biochem. 2002; 85:629–639. [PubMed: 11968003]

Bocci G, Francia G, Man S, Lawler J, Kerbel RS. Thrombospondin 1, a mediator of the antiangiogenic effects of low-dose metronomic chemotherapy. Proc Natl Acad Sci USA. 2003; 100:12917–12922. [PubMed: 14561896]

Bornstein P. Thrombospondins: Structure and regulation of expression. FASEB J. 1992; 6:3290–3299. [PubMed: 1426766]

Bu G, Marzolo MP. Role of rap in the biogenesis of lipoprotein receptors. Trends Cardiovasc Med. 2000; 10:148–155. [PubMed: 11239794]

Castellon R, Hamdi HK, Sacerio I, Aoki AM, Kenney MC, Ljubimov AV. Effects of angiogenic growth factor combinations on retinal endothelial cells. Exp Eye Res. 2002; 74:523–535. [PubMed: 12076096]

Cursiefen C, Masli S, Ng TF, Dana MR, Bornstein P, Lawler J, Streilein JW. Roles of thrombospondin-1 and-2 in regulating corneal and iris angiogenesis. Invest Ophthalmol Vis Sci. 2004; 45:1117–1124. [PubMed: 15037577]

Dawson DW, Pearce SF, Zhong R, Silverstein RL, Frazier WA, Bouck NP. CD36 mediates the in vitro inhibitory effects of thrombospondin-1 on endothelial cells. J Cell Biol. 1997; 138:707–717. [PubMed: 9245797]

Detmar M. Tumor angiogenesis. J Investig Dermatol Symp Proc. 2000; 5:20–23.

Doll JA, Reiher FK, Crawford SE, Pins MR, Campbell SC, Bouck NP. Thrombospondin-1, vascular endothelial growth factor and fibroblast growth factor-2 are key functional regulators of angiogenesis in the prostate. Prostate. 2001; 49:293–305. [PubMed: 11746276]

Emonard H, Bellon G, Troeberg L, Berton A, Robinet A, Henriet P, Marbaix E, Kirkegaard K, Patthy L, Eeckhout Y, Nagase H, Hornebeck W, Courtoy PJ. Low density lipoprotein receptor-related protein mediates endocytic clearance of pro-MMP-2. TIMP-2 complex through a thrombospondin-independent mechanism. J Biol Chem. 2004; 279:54944–54951. [PubMed: 15489233]

Ferrara N. Vascular endothelial growth factor: Basic science and clinical progress. Endocr Rev. 2004; 25:581–611. [PubMed: 15294883]

Folkman J. The role of angiogenesis in tumor growth. Semin Cancer Biol. 1992; 3:65–71. [PubMed: 1378311]

Fontana A, Filleur S, Guglielmi J, Frappart L, Bruno-Bossio G, Boissier S, Cabon F, Clezardin P. Human breast tumors override the antiangiogenic effect of stromal thrombospondin-1 in vivo. Int J Cancer. 2005; 116:686–691. [PubMed: 15838828]

Fraser HM, Wulff C. Angiogenesis in the primate ovary. Reprod Fertil Dev. 2001; 13:557–566. [PubMed: 11999306]

Gerber HP, McMurtrey A, Kowalski J, Yan M, Keyt BA, Dixit V, Ferrara N. Vascular endothelial growth factor regulates endothelial cell survival through the phosphatidylinositol 3′-kinase/Akt signal transduction pathway. Requirement for Flk-1/KDR activation. 1998; 273:30336–30343.

Godyna S, Liau G, Popa I, Stefansson S, Argraves WS. Identification of the low density lipoprotein receptor-related protein (LRP) as an endocytic receptor for thrombospondin-1. J Cell Biol. 1995; 129:1403–1410. [PubMed: 7775583]

Gonzalez F, Rueda A, Sevilla I, Alonso L, Villarreal V, Torres E, Alba E. Shift in the balance between circulating thrombospondin-1 and vascular endothelial growth factor in cancer patients: Relationship to platelet alpha-granule content and primary activation. Int J Biol Markers. 2004; 19:221–228. [PubMed: 15503824]

Greenaway J, Connor K, Pedersen HG, Coomber BL, LaMarre J, Petrik J. Vascular endothelial growth factor and its receptor, Flk-1/KDR, are cytoprotective in the extravascular compartment of the ovarian follicle. Endocrinology. 2004; 145:2896–2905. [PubMed: 14988387]

Greenaway J, Gentry PA, Feige JJ, LaMarre J, Petrik J. Thrombospondin and vascular endothelial growth factor are cyclically expressed in an inverse pattern during bovine ovarian follicle development. Biol Reprod. 2005; 72:1071–1078. [PubMed: 15616224]

Guo NH, Krutzsch HC, Inman JK, Shannon CS, Roberts DD. Antiproliferative and antitumor activities of D-reverse peptides derived from the second type-1 repeat of thrombospondin-1. J Pept Res. 1997; 50:210–221. [PubMed: 9309585]

Gupta K, Gupta P, Wild R, Ramakrishnan S, Hebbel RP. Binding and displacement of vascular endothelial growth factor (VEGF) by thrombospondin: Effect on human microvascular endothelial cell proliferation and angiogenesis. Angiogenesis. 1999; 3:147–158. [PubMed: 14517432]

Inoki I, Shiomi T, Hashimoto G, Enomoto H, Nakamura H, Makino K, Ikeda E, Takata S, Kobayashi K, Okada Y. Connective tissue growth factor binds vascular endothelial growth factor (VEGF) and inhibits VEGF-induced angiogenesis. FASEB J. 2002; 16:219–221. [PubMed: 11744618]

Jia H, Bagherzadeh A, Bicknell R, Duchen MR, Liu D, Zachary I. Vascular endothelial growth factor (VEGF)-D and VEGF-A differentially regulate KDR-mediated signaling and biological function in vascular endothelial cells. J Biol Chem. 2004; 279:36148–36157. [PubMed: 15215251]

Jimenez B, Volpert OV, Crawford SE, Febbraio M, Silverstein RL, Bouck NP. Signals leading to apoptosis-dependent inhibition of neovascularization by thrombospondin-1. Nat Med. 2000; 6:41–48. [PubMed: 10613822]

Jonard S, Robert Y, Dewailly D. Revisiting the ovarian volume as a diagnostic criterion for polycystic ovaries. Hum Reprod. 2005; 20:2893–2898. [PubMed: 16006474]

Kerbel RS, Kamen BA. The anti-angiogenic basis of metronomic chemotherapy. Nat Rev Cancer. 2004; 4:423–436. [PubMed: 15170445]

Kwak C, Jin RJ, Lee C, Park MS, Lee SE. Thrombospondin-1, vascular endothelial growth factor expression and their relationship with p53 status in prostate cancer and benign prostatic hyperplasia. BJU Int. 2002; 89:303–309. [PubMed: 11856116]

Laithwaite JE, Benn SJ, Marshall WS, FitzGerald DJ, LaMarre J. Divergent Pseudomonas exotoxin A sensitivity in normal and transformed liver cells is correlated with low-density lipoprotein receptor-related protein expression. Toxicon. 2001; 39:1283–1290. [PubMed: 11384715]

Lawler J. Thrombospondin-1 as an endogenous inhibitor of angiogenesis and tumor growth. J Cell Mol Med. 2002; 6:1–12. [PubMed: 12003665]

Lawler J, Detmar M. Tumor progression: The effects of thrombospondin-1 and -2. Int J Biochem Cell Biol. 2004; 36:1038–1045. [PubMed: 15094119]

Lawler J, Sunday M, Thibert V, Duquette M, George EL, Rayburn H, Hynes RO. Thrombospondin-1 is required for normal murine pulmonary homeostasis and its absence causes pneumonia. J Clin Invest. 1998; 101:982–992. [PubMed: 9486968]

Lawler JM, Miao WM, Duquette M, Bouck N, Bronson RT, Hynes RO. Thrombospondin-1 gene expression affects survival and tumor spectrum of p53-deficient mice. Am J Pathol. 2001; 159:1949–1956. [PubMed: 11696456]

Lazic A, Dolmer K, Strickland DK, Gettins PG. Structural organization of the receptor associated protein. Biochemistry. 2003; 42:14913–14920. [PubMed: 14674767]

Li ZD, Bork JP, Krueger B, Patsenker E, Schulze-Krebs A, Hahn EG, Schuppan D. VEGF induces proliferation, migration, and TGF-beta1 expression in mouse glomerular endothelial cells via mitogen-activated protein kinase and phosphatidylinositol 3-kinase. Biochem Biophys Res Commun. 2005; 334:1049–1060. [PubMed: 16039615]

Manabe N, Goto Y, Matsuda-Minehata F, Inoue N, Maeda A, Sakamaki K, Miyano T. Regulation mechanism of selective atresia in porcine follicles: Regulation of granulosa cell apoptosis during atresia. J Reprod Dev. 2004; 50:493–514. [PubMed: 15514456]

Margosio B, Marchetti D, Vergani V, Giavazzi R, Rusnati M, Presta M, Taraboletti G. Thrombospondin 1 as a scavenger for matrix-associated fibroblast growth factor 2. Blood. 2003; 102:4399–4406. [PubMed: 12947001]

Mikhailenko I, Kounnas MZ, Strickland DK. Low density lipoprotein receptor-related protein/alpha 2-macroglobulin receptor mediates the cellular internalization and degradation of thrombospondin. A process facilitated by cell-surface proteoglycans. J Biol Chem. 1995; 270:9543–9549. [PubMed: 7721883]

Mikhailenko I, Krylov D, Argraves KM, Roberts DD, Liau G, Strickland DK. Cellular internalization and degradation of thrombospondin-1 is mediated by the amino-terminal heparin binding domain (HBD). High affinity interaction of dimeric HBD with the low density lipoprotein receptor-related protein. J Biol Chem. 1997; 272:6784–6791. [PubMed: 9045712]

Moestrup SK, Gliemann J, Pallesen G. Distribution of the alpha 2-macroglobulin receptor/low density lipoprotein receptor-related protein in human tissues. Cell Tissue Res. 1992; 269:375–382. [PubMed: 1423505]

Neels JG, van Den Berg BM, Lookene A, Olivecrona G, Pannekoek H, van Zonneveld AJ. The second and fourth cluster of class A cysteine-rich repeats of the low density lipoprotein receptor-related protein share ligand-binding properties. J Biol Chem. 1999; 274:31305–31311. [PubMed: 10531329]

Nyberg P, Xie L, Kalluri R. Endogenous inhibitors of angiogenesis. Cancer Res. 2005; 65:3967–3979. [PubMed: 15899784]

Nykjaer A, Willnow TE. The low-density lipoprotein receptor gene family: A cellular Swiss army knife? Trends Cell Biol. 2002; 12:273–280. [PubMed: 12074887]

Pauli SA, Tang H, Wang J, Bohlen P, Posser R, Hartman T, Sauer MV, Kitajewski J, Zimmermann RC. The vascular endothelial growth factor (VEGF)/VEGF receptor 2 pathway is critical for blood vessel survival in corpora lutea of pregnancy in the rodent. Endocrinology. 2005; 146:1301–1311. [PubMed: 15591152]

Petrik JJ, Gentry PA, Feige JJ, LaMarre J. Expression and localization of thrombospondin-1 and -2 and their cell-surface receptor, CD36, during rat follicular development and formation of the corpus luteum. Biol Reprod. 2002; 67:1522–1531. [PubMed: 12390884]

Scharovsky OG, Binda MM, Rozados VR, Bhagat S, Cher M, Bonfil RD. Angiogenic and antiangiogenic balance regulates concomitant antitumoral resistance. Clin Exp Metastasis. 2004; 21:177–183. [PubMed: 15168735]

Sengupta K, Banerjee S, Saxena NK, Banerjee SK. Thombospondin-1 disrupts estrogen-induced endothelial cell proliferation and migration and its expression is suppressed by estradiol. Mol Cancer Res. 2004; 2:150–158. [PubMed: 15037654]

Shen GH, Ghazizadeh M, Kawanami O, Shimizu H, Jin E, Araki T, Sugisaki Y. Prognostic significance of vascular endothelial growth factor expression in human ovarian carcinoma. Br J Cancer. 2000; 83:196–203. [PubMed: 10901370]

Strickland DK, Gonias SL, Argraves WS. Diverse roles for the LDL receptor family. Trends Endocrinol Metab. 2002; 13:66–74. [PubMed: 11854021]

Sund M, Hamano Y, Sugimoto H, Sudhakar A, Soubasakos M, Yerramalla U, Benjamin LE, Lawler J, Kieran M, Shah A, Kalluri R. Function of endogenous inhibitors of angiogenesis as endothelium-specific tumor suppressors. Proc Natl Acad Sci USA. 2005; 102:2934–2939. [PubMed: 15710885]

Tsafriri A. Ovulation as a tissue remodelling process. Proteolysis and cumulus expansion. Adv Exp Med Biol. 1995; 377:121–140. [PubMed: 7484419]

Tsukada K, Matsushima T, Yamanaka N. Neovascularization of the corpus luteum of rats during the estrus cycle. Pathol Int. 1996; 46:408–416. [PubMed: 8869992]

Vacca A, Ria R, Ribatti D, Semeraro F, Djonov V, Di Raimondo F, Dammacco F. A paracrine loop in the vascular endothelial growth factor pathway triggers tumor angiogenesis and growth in multiple myeloma. Haematologica. 2003; 88:176–185. [PubMed: 12604407]

Valdez KE, Cuneo SP, Turzillo AM. Regulation of apoptosis in the atresia of dominant bovine follicles of the first follicular wave following ovulation. Reproduction. 2005; 130:71–81. [PubMed: 15985633]

Wang S, Wu Z, Sorenson CM, Lawler J, Sheibani N. Thrombospondin-1-deficient mice exhibit increased vascular density during retinal vascular development and are less sensitive to hyperoxia-mediated vessel obliteration. Dev Dyn. 2003; 228:630–642. [PubMed: 14648840]

Wang S, Herndon ME, Ranganathan S, Godyna S, Lawler J, Argraves WS, Liau G. Internalization but not binding of thrombospondin-1 to low density lipoprotein receptor-related protein-1 requires heparan sulfate proteoglycans. J Cell Biochem. 2004; 91:766–776. [PubMed: 14991768]

Wiltbank MC, Dysko RC, Gallagher KP, Keyes PL. Relationship between blood flow and steroidogenesis in the rabbit corpus luteum. J Reprod Fertil. 1988; 84:513–520. [PubMed: 3199370]

Wulff C, Wilson H, Wiegand SJ, Rudge JS, Fraser HM. Prevention of thecal angiogenesis, antral follicular growth, and ovulation in the primate by treatment with vascular endothelial growth factor Trap R1R2. Endocrinology. 2002; 143:2797–2807. [PubMed: 12072415]

Yamamoto M, Ikeda K, Ohshima K, Tsugu H, Kimura H, Tomonaga M. Increased expression of low density lipoprotein receptor-related protein/alpha2-macroglobulin receptor in human malignant astrocytomas. Cancer Res. 1997; 57:2799–2805. [PubMed: 9205092]

Yang Z, Strickland DK, Bornstein P. Extracellular matrix metalloproteinase 2 levels are regulated by the low density lipoprotein-related scavenger receptor and thrombospondin 2. J Biol Chem. 2001; 276:8403–8408. [PubMed: 11113133]

Yano K, Oura H, Detmar M. Targeted overexpression of the angiogenesis inhibitor thrombospondin-1 in the epidermis of transgenic mice prevents ultraviolet-B-induced angiogenesis and cutaneous photo-damage. J Invest Dermatol. 2002; 118:800–805. [PubMed: 11982756]

Zimmermann RC, Xiao E, Husami N, Saue MV, Lobo R, Kitajewski J, Ferin M. Short-term administration of antivascular endothelial growth factor antibody in the late follicular phase delays follicular development in the rhesus monkey. J Clin Endocrinol Metab. 2001; 86:768–772. [PubMed: 11158044]

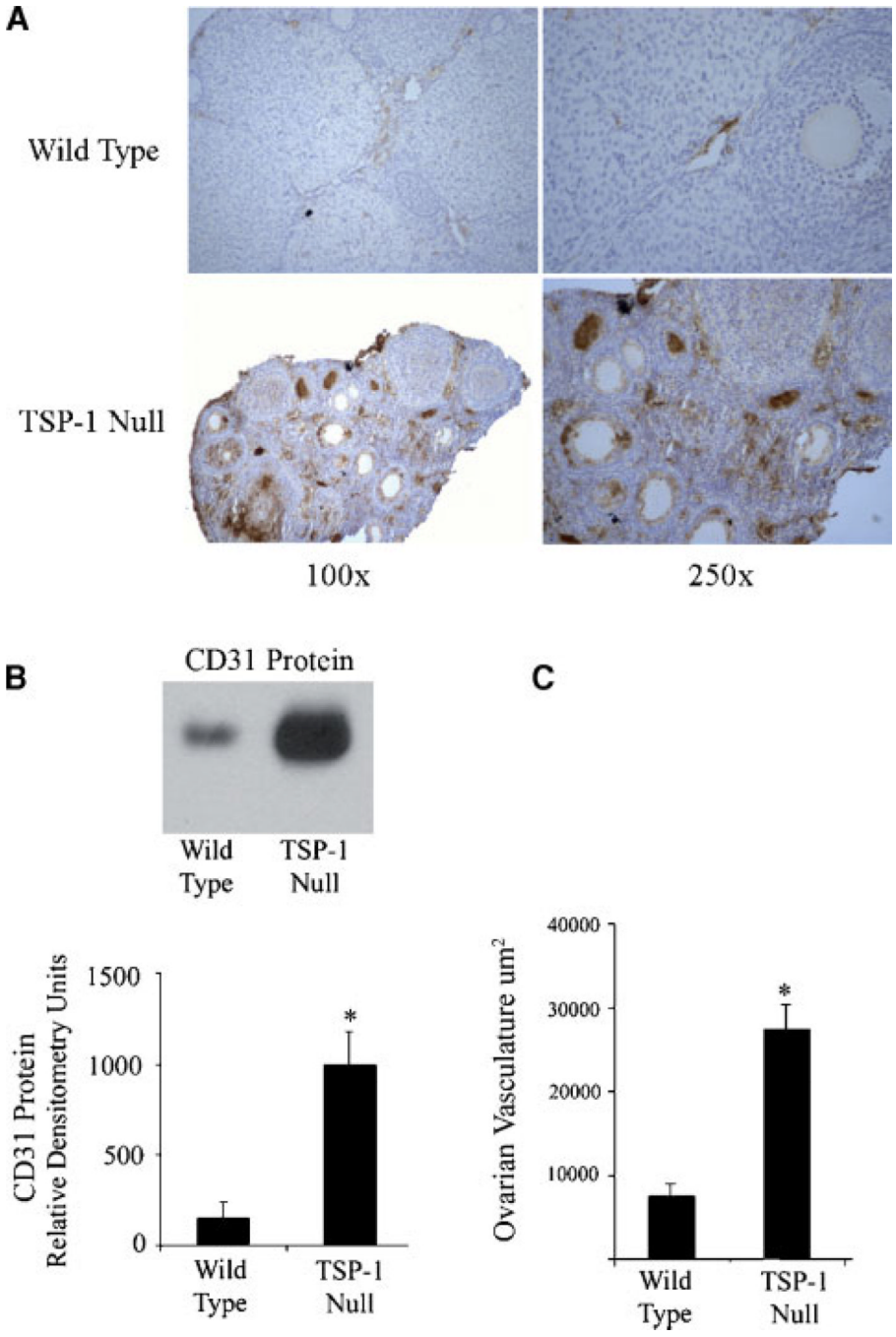

Fig. 1. Expression of CD31 and quantification of vessel density in ovaries from wild-type and TSP-1-nullmice

A: Ovaries from wild-type and TSP-1 null mice were immunostained for CD31 (brown stain). Ovaries of wild type mice demonstrated peri-follicular, thecal, and luteal immunopositive blood vessels. TSP-1-null mice exhibited increased expression of CD31, with the presence of large CD31-positive blood vessels. **B**: Western blot; there was a significant increase in CD31 protein in ovaries from TSP-1-null versus wild-type mice. **C**: Ovarian vessel density was calculated as the total area of CD31-positive blood vessels in wild-type and TSP-1-null mice. TSP-1 null ovaries had a significantly elevated blood vessel

density, compared to wild-type controls. For the Western blot graph, * denotes a statistical difference in CD31 protein compared to wild-type controls ($P < 0.05$).

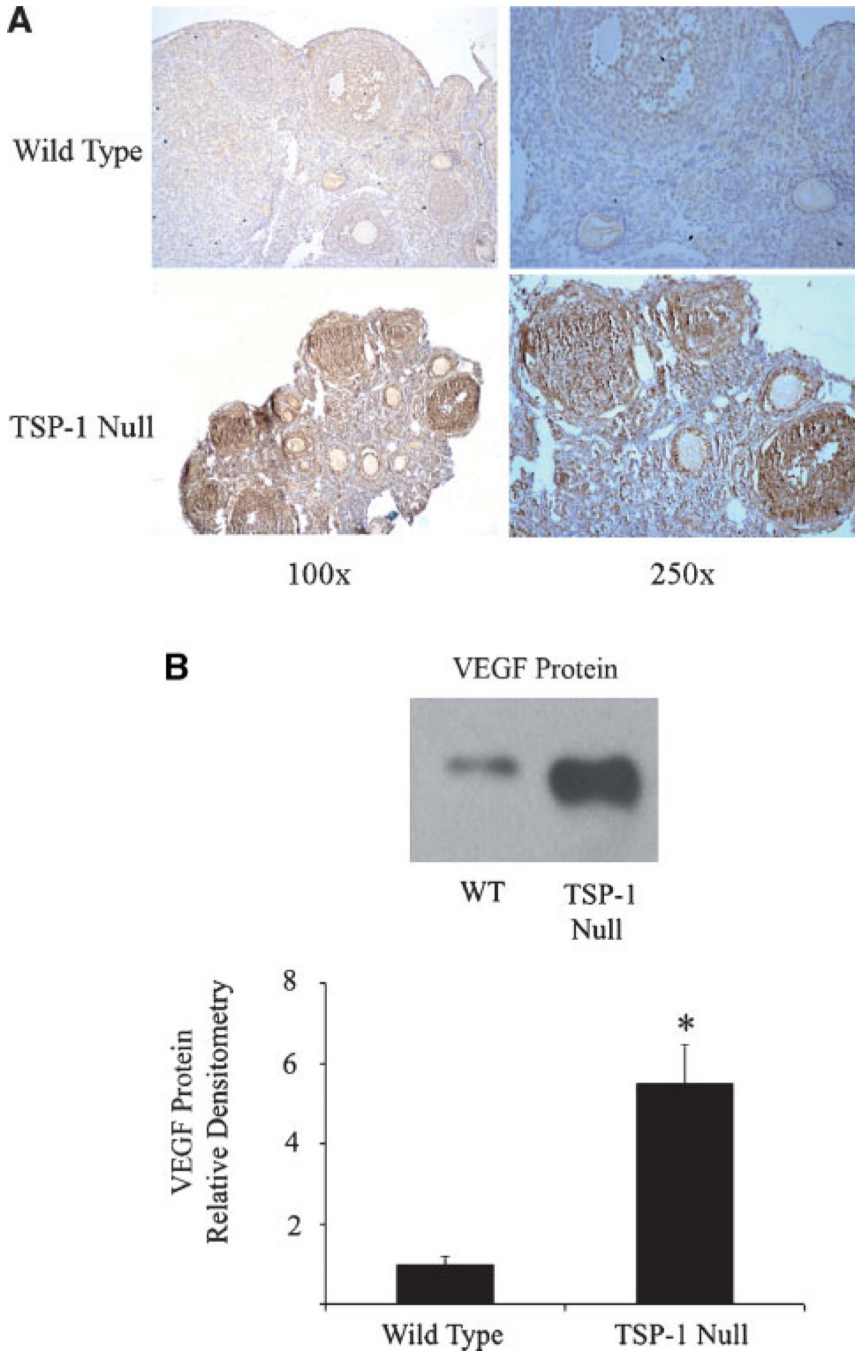

Fig. 2. Expression of VEGF in ovaries from wild-type and TSP-1-null mice

A: Ovaries from TSP-1-null mice exhibited an increase in VEGF-positive cells (brown stain) that were localized to the corpus luteum, granulosa/theca cells of the follicle, and endothelial cells. **B**: There was a significant increase VEGF protein in TSP-1-null ovaries compared to wild-type ovaries, as measured by Western blotting. For the Western blot graph, * denotes a statistically significant difference in VEGF protein compared to wild-type controls ($P < 0.05$).

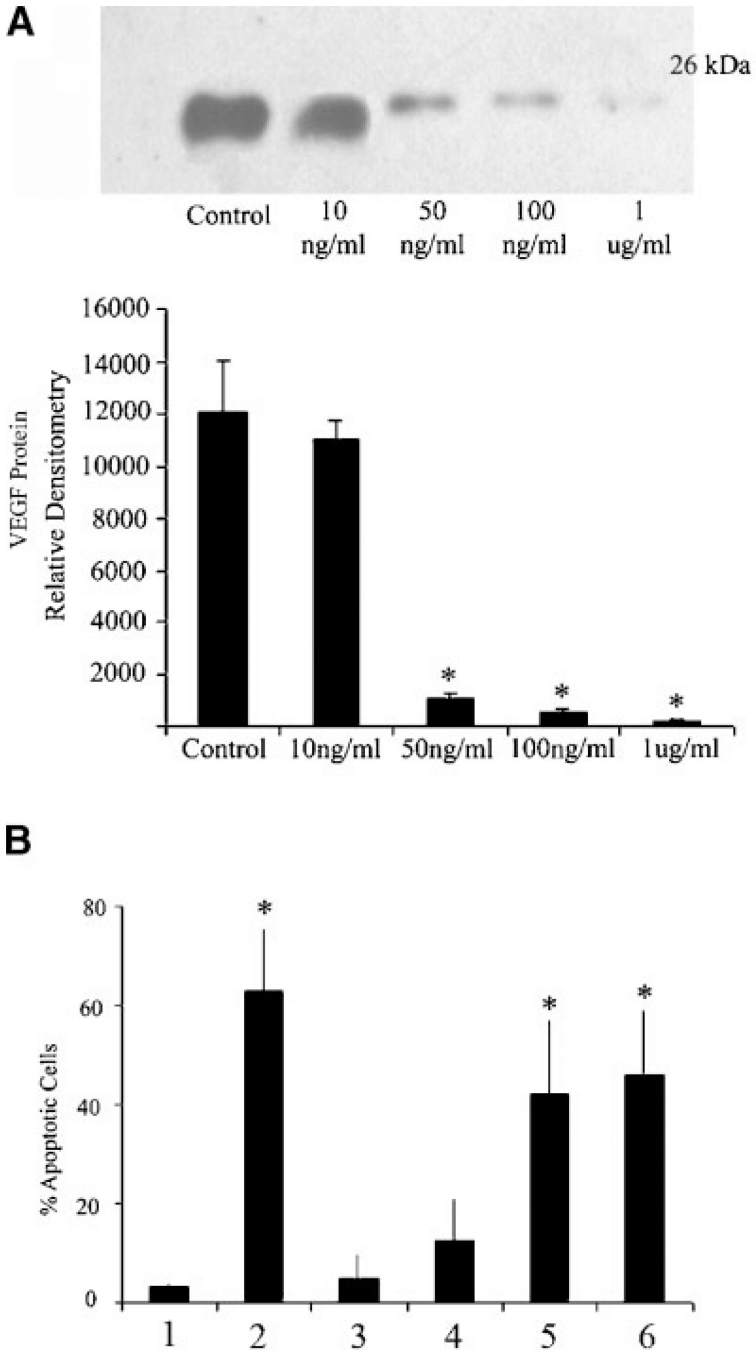

Fig. 3. TSP-1 treatment of SIGC inhibits VEGF protein expression and induces apoptosis

A: Western blot analysis of VEGF protein from SIGC treated for 24 h with increasing amounts of purified TSP-1. Graph represents densitometric analysis of VEGF protein from three different in vitro experiments (mean ± SEM). **B**: Percent apoptosis in granulosa cells subjected to TNFα challenge in the absence or presence of variable concentrations of TSP-1. All cultures were performed in serum-free media. Lane 1: No treatment; Lane 2: 100 ng/ml TNFα; Lane 3: 100 ng/ml TNFα + 50 ng/ml VEGF + 10 ng/ml TSP-1; Lane 4: 100 ng/ml TNFα + 50 ng/ml VEGF + 50 ng/ml TSP-1; Lane 5: 100 ng/ml TNFα + 50 ng/ml VEGF + 100 ng/ml TSP-1; Lane 5: 100 ng/ml TNFα + 50 ng/ml VEGF + 1 μg/ml TSP-1. *

denotes statistically different from serum free control (Lane 1) ($P < 0.05$) (n = 3 experiments).

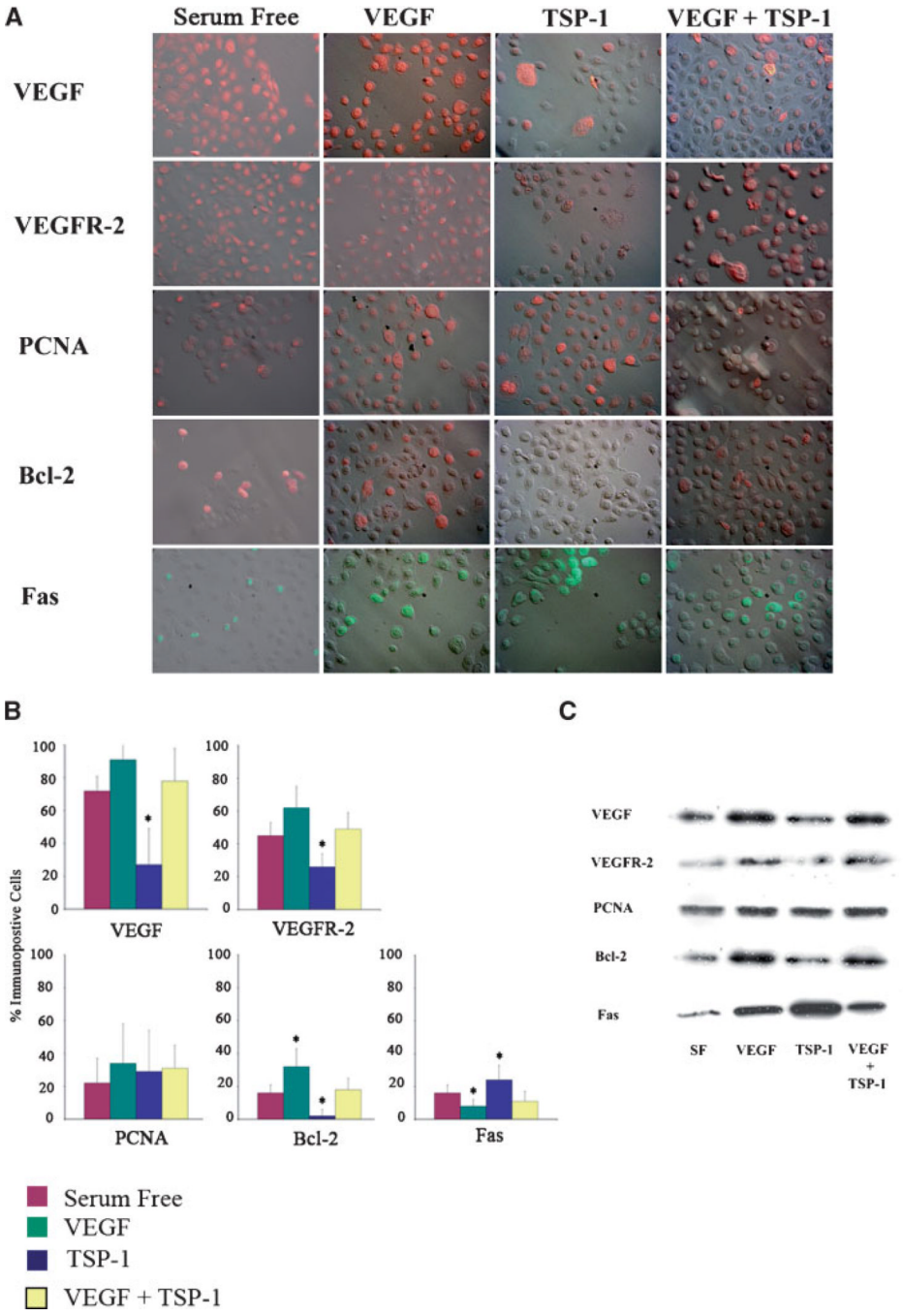

Fig. 4. Expression of proteins relevant to proliferation and apoptosis in response to VEGF, TSP-1, or combination treatment

A: Relief contrast overlay immunofluorescence images of untreated granulosa cells or after treatment with 50 ng/ml VEGF, 100 ng/ml TSP-1 or a combination of 50 ng/ml VEGF and 100 ng/ml TSP-1. **B**: Quantification of the percentage of immunopositive in vitro cells from (A). Graphs represent four replicate experiments (mean ± SEM). **C**: Representative (of four replicate) western blots of proteins isolated from granulosa cells treated with VEGF, TSP-1, or both. A decrease in cytoprotective VEGF, VEGR2, and bcl-2 is observed after treatment with 100 ng/ml TSP-1 compared to treatment with 50 ng/ml VEGF. Conversely, an increase

in pro-apoptotic Fas occurs following treatment with TSP-1. * denotes statistically different from serum free controls ($P > 0.05$).

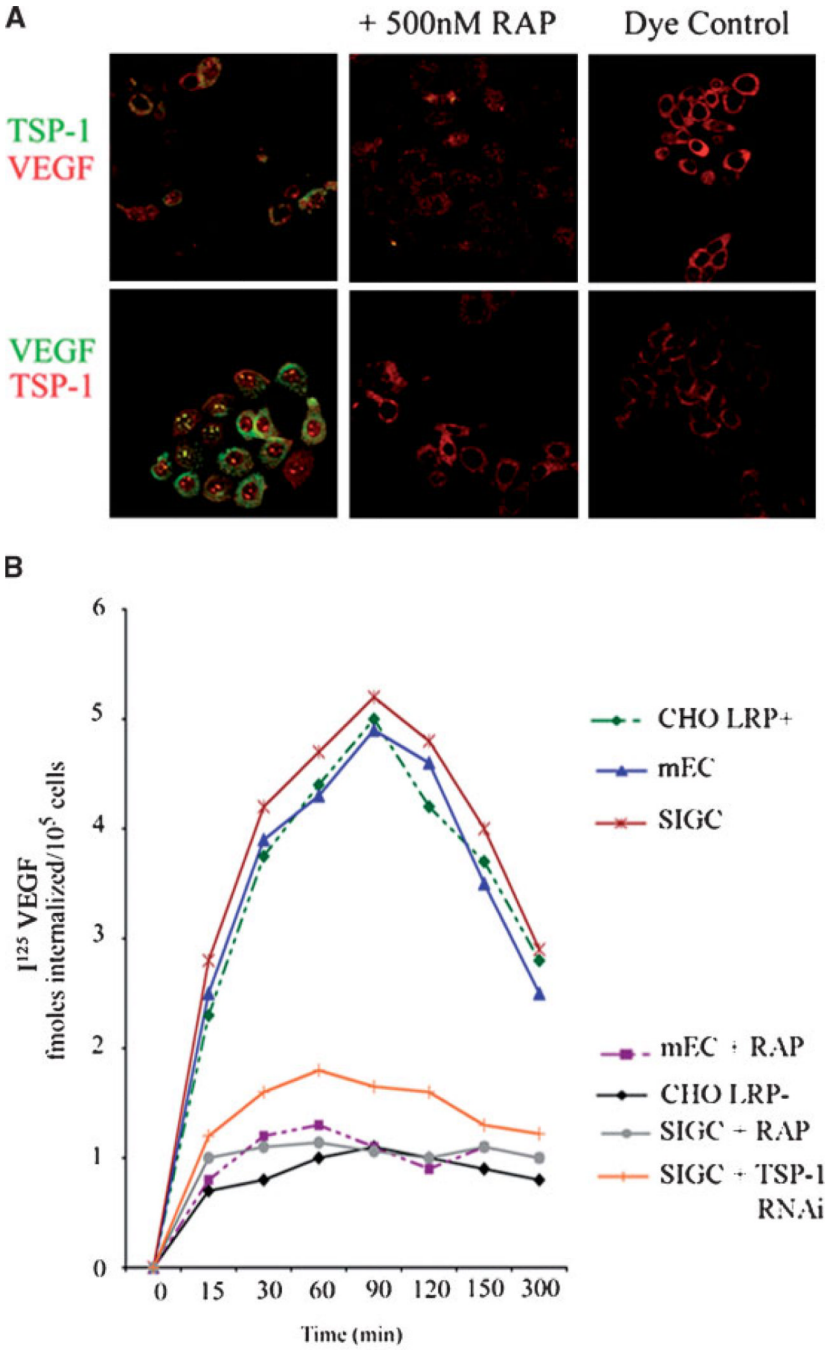

Fig. 5. Binding and internalization of TSP-1/VEGF by the LRP receptor

A: Immunofluorescent co-localization of TSP-1 and VEGF in the absence or presence of the LRP-1 antagonist RAP. Cells were treated for 6 h with purified VEGF or TSP-1 labeled with AlexaFluor 488 dye (green stain). Co-staining for TSP-1 or VEGF was performed with an AlexaFluor 594 conjugated antibody (red stain). Reciprocal experiments are shown. A sample containing only AlexaFluor dye (no protein) is shown as negative control. **B**: ^{125}I labeled VEGF is internalized by LRP-1-expressing Chinese hamster ovary (CHO) cells and native murine endothelial (mEC) and granulosa cells (SIGC), but not LRP-1-deficient CHO cells or by SIGC and mEC treated with 500 nM RAP, or by SIGC treated with TSP-1 siRNA. CHO, SIGC, and mEC were plated into 12-well dishes 24 h prior to the assay. 1

nM ^{125}I-Labeled VEGF was added to LRP-positive and -negative CHO cells, to SIGC and mEC in the presence or absence of 500 nM RAP, and to SIGC treated with TSP-1 siRNA. At the indicated times, the amount of internalized radioactivity was determined. Each data point represents the average of duplicate assays (n = 3).

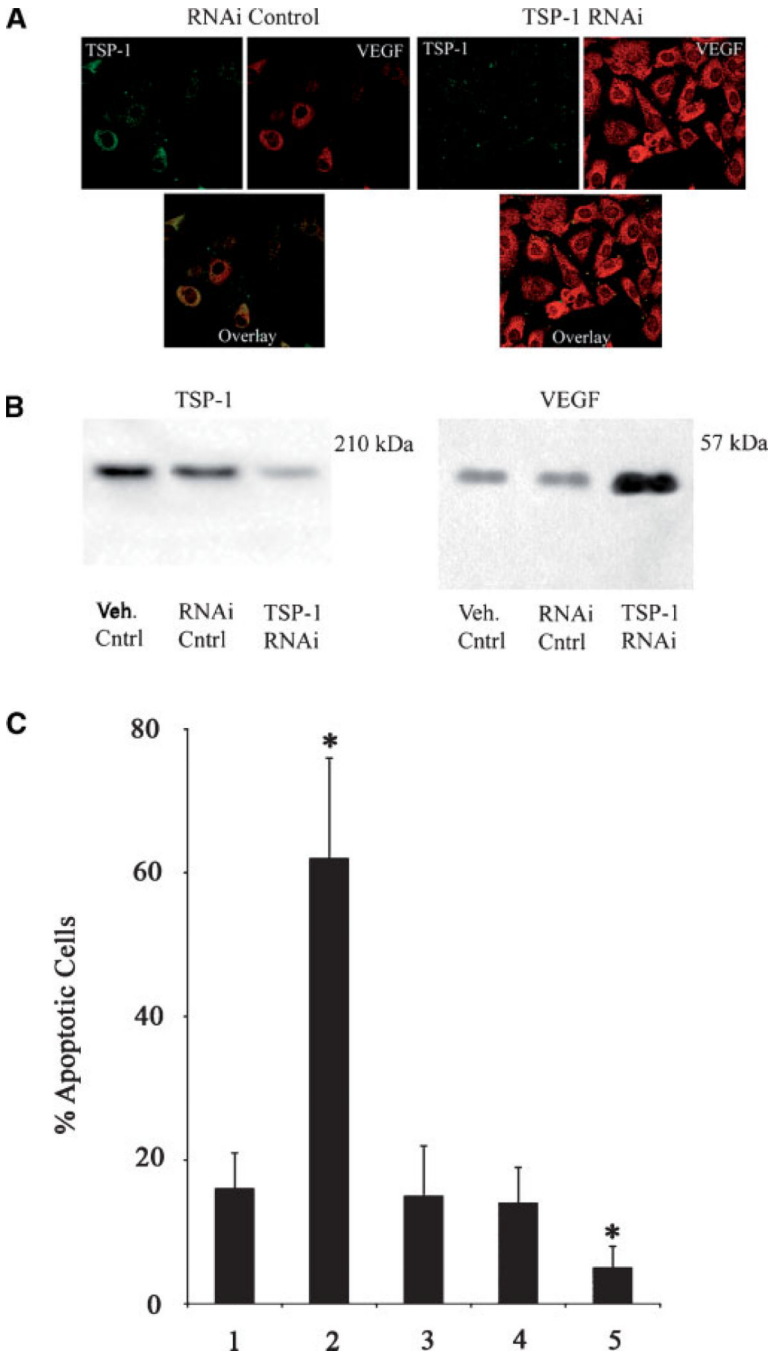

Fig. 6. TSP-1 knockdown results in increased VEGF expression and reduced apoptosis

A: Immunofluorescence for TSP-1 (green) and VEGF (red) SIGC treated with scrambled sequence (RNAi control) or TSP-1 siRNA. Images are acquired with identical acquisition settings. **B**: Western blot analysis of TSP-1 and VEGF in control and TSP-1 siRNA treated SIGC. **C**: Percent apoptosis in untreated, and cyokine-challenged SIGC in the presence or absence of controls or TSP-1 siRNA. All cultures were performed in serum free media. Lane 1: No treatment; Lane 2: 100 ng/ml TNFα; Lane 3: 100 ng/ml TNFα + 50 ng/ml VEGF + vehicle control; Lane 4: 100 ng/ml TNFα + 50 ng/ml VEGF + RNAi control; Lane 5: 100 ng/ml TNFα + 50 ng/ml VEGF + TSP-1 RNAi. * denotes statistically different from serum free control (Lane 1) ($P < 0.05$) (n = 3 experiments).

TABLE 1

Follicle morphology of wild-type and TSP-1-null mice

	Follicle number		Follicle diameter (μm)	
	Pre-antral	**Antral**	**Pre-antral**	**Antral**
Wild-type	21 ± 4	10 ± 3	31 ± 6	44 ± 6
TSP-1-null	28 ± 5 *	17 ± 5 *	28 ± 5	36 ± 4 *

Total follicle number and follicle diameters were calculated from a minimum of 10 ovaries at the pre-antral and antral stages of development from wild-type and TSP-1-null mice.

* denotes statistically significant difference ($P < 0.05$) between TSP-1-null and wild-type group.